Effect of surface anchoring energy on electro-optic characteristics of a fringe-field switching liquid crystal cell

2015 J. Phys. D: Appl. Phys. 48 465506

(http://iopscience.iop.org/0022-3727/48/46/465506)

IOP Publishing Journal of Physics D: Applied Physics
J. Phys. D: Appl. Phys. **48** (2015) 465506 (9pp) doi:10.1088/0022-3727/48/46/465506

Effect of surface anchoring energy on electro-optic characteristics of a fringe-field switching liquid crystal cell

Jin Hyun Kim[1,4], Wan Seok Kang[2,3,4], Han Sol Choi[1], Kiwoong Park[2], Joong Hee Lee[1], Sangho Yoon[3], Sukin Yoon[3], Gi-Dong Lee[2] and Seung Hee Lee[1]

[1] Applied Materials Institute for BIN Convergence, Department of BIN Convergence Technology and Department of Polymer-Nano Science and Technology, Chonbuk National University, Jeonju, Jeonbuk 561–756, Korea
[2] Department of Electronics Engineering, Dong-A University, Pusan 604–714, Korea
[3] Sanayisystem Co. Ltd., Incheon 402–711, Korea

E-mail: gdlee@dau.ac.kr and lshl@chonbuk.ac.kr

Received 4 August 2015, revised 20 September 2015
Accepted for publication 28 September 2015
Published 22 October 2015

Abstract
Surface anchoring strength of the alignment layer on liquid crystal (LC) determines electro-optic characteristics in the LC devices. This paper investigates how azimuthal and polar anchoring strength affects the electro-optic performance of a fringe-field switching (FFS) mode associated with electrode structure, cell gap and dielectric anisotropy of the LC by numerical simulation. Our important findings in the FFS mode are that both azimuthal and polar anchoring energy can considerably affect the operating voltage and also maximum transmittance when using a LC with positive dielectric anisotropy; however, when using a LC with negative dielectric anisotropy only azimuthal anchoring energy affects electro-optic characteristics. The study proposes an optimal design of an alignment layer for maximizing transmittance in the FFS mode.

Keywords: liquid crystal, fringe field switching, surface anchoring energy

(Some figures may appear in colour only in the online journal)

1. Introduction

Nowadays, liquid crystal displays (LCDs) are widely used in all display applications owing to the characteristics such as lightness, thinness, low power consumption, and superior image quality. For better optical performances, researchers have been developing the advanced liquid crystal (LC) mode such as twisted nematic, in-plane switching, multi-domain vertical alignment, and fringe-field switching (FFS) [1–5]. The initial alignment of LC molecules in these advanced LC modes in common can be realized by rubbing method which has some advantages such as fast and simple working process. In addition, this process can provide superior anchoring energy to the LC molecules on the polyimide (PI) layer. The surface anchoring energy of an alignment layer contributes to the optical performance of LCDs such as operating voltage, decay time, transmittance and phase transition for bi-stable state [6, 7]. However, direct contact for initial LC alignment between a PI layer and rubbing roller seriously results in damages from static electricity and residual materials such as dust and scratches on a PI layer. Also, rubbing mura and rubbing-related light leakage in the dark state exist because of non-rubbed region near electrodes and nonuniformity of the anchoring strength from display position to position so that the contrast ratio of the device is seriously decreased and also the nonuniformity in grey scale is generated [8].

In order to overcome the above-mentioned problems, various non-contact alignment methods have been developed [9–12]. Among them is a photo-decomposition type which is commercialized now [13]. In this case, a photosensitive

[4] Co-first author with the same contribution to this work.

polymer is known to produce homogeneous alignment of the LC molecules perpendicular to the linearly polarized (LP) ultra-violet (UV) light because the LPUV light breaks the polymer backbones lying parallel to the UV polarization at the surface, revealing the photoalignment effect [12]. However, including the LPUV, most of the non-contact alignment method represents relatively weak azimuthal and polar anchoring energy compared to those with mechanical rubbing method [14].

In the FFS mode, the transmittance is directly concerned with cell parameters such as cell retardation [15, 16], sign and magnitude of LC's dielectric anisotropy [17], cell gap [18, 19] and electrode width and distance between electrodes [20, 21]. Up to our knowledge, detail studies how each azimuthal and polar anchoring energy affects electro-optics of a FFS cell have not been reported. Considering non-contact method for LC alignment of a FFS LC cell which is commercialized now, this paper investigates how the magnitude of anchoring energy affects electro-optical performance of the FFS LC cell in different cell conditions.

2. Switching principle of the FFS cell and simulation conditions

Figure 1 shows a cross-sectional view of the schematic cell structure and LC orientation in voltage off and on states in a FFS cell, in which the common electrode and the patterned pixel electrode with width (w) and distance (l) between them exist on the bottom substrate. The passivation layer is inserted between two electrodes, in which the electrodes are consisted of transparent materials. The LCs are homogeneously aligned in an initial state where the optical axis of the LC is parallel to one of the crossed polarizer axis. Therefore, the LC cell can achieve the dark state in the absence of an electric field. By applying a voltage to the LC cell, the fringe electric (E)-field with both horizontal (E_y) and vertical (E_z) components is generated between patterned and common electrodes. The dielectric and elastic torque based on the fringe E-field are able to rotate LC directors in the bottom and middle LC layer over whole electrode surface depending on an electrode position so that the optical transmittance is increased. However, the optical transmittance of a FFS mode is periodically oscillated along electrode direction [22]. In general, position C (at the edge of electrodes) in a FFS mode represents stronger horizontal E-field than other positions whereas more intensive E_z component is induced at position B (between the centre and the edge of the electrode). Both E_y and E_z are zero at the middle of the electrode (position A). Consequently, at position C, the LCs are mostly rotated near bottom surface due to strong E_y. The intensity of E-field along z-axis continuously decreases from bottom to the top substrate. Therefore, the LC configuration at position C is similar to twisted nematic LC cell and light modulation occurs because of polarization rotation. In contrast, LC molecules at position A are twisted by elastic torque of its neighbouring molecules. However, the LCs on each surface layer at position A are not fully rotated due to the surface anchoring energy and weak E-field components whereas the LCs in the middle of LC layer can be aligned to y-direction. The final LC configuration at position A is similar to an IPS LC cell whose light modulation depends on the phase retardation effect [23]. Consequently, the normalized light transmittance in FFS cell using a positive dielectric LC material is determined by the following equation (1) [18]:

$$\frac{T}{T_0} = A\sin^2\!\left(\frac{B\pi d\Delta n}{\lambda}\right) + C\left(1 - \frac{\sin^2\!\left(\frac{\pi}{2}\sqrt{1+\left(\frac{2Dd\Delta n}{\lambda}\right)^2}\right)}{1-\left(\frac{2Dd\Delta n}{\lambda}\right)^2}\right), \tag{1}$$

where A, B, C and D are fitting parameters, d is a cell gap, Δn is a birefringence of LC layer and λ is the wavelength of the incident light. The first and second term are related to the phase retardation and polarization rotation effect, respectively.

Another interesting point in the FFS mode is that the homogeneously aligned LCs in an initial state is deformed along the fringe-field direction so that the tilt as well as twist reorientation of LCs does occur with bias voltage, implying that magnitude of both polar (W_θ) and azimuthal (W_φ) surface anchoring energy (W) at the interface of LC and an alignment layer might affect electro-optic characteristics of the FFS mode.

In order to investigate the effect on surface anchoring energy of an alignment layer, potential distribution and LC director configuration as function of cell parameters such as electrode pitch, cell gap and type of a LC material are calculated. We performed a computer simulation using the commercially available software '*TechWiz LCD*' (Sanayisystem, Korea), where the dynamics of LC director is simulated based on *Eriksen–Leslie* theory [24]. The LC director configuration of an LC cell is calculated by minimizing the Gibbs free energy [25]. The Gibbs free energy is composed of three energy terms as following equation (2):

$$F_{\text{Gibbs free energy}} = F_{\text{elastic energy}} + F_{\text{electric energy}} + F_{\text{surface anchoring energy}}. \tag{2}$$

Generally, the third term for LC molecules on alignment layers is often omitted because LC on the alignment layer assumes to be strongly anchored such that surface anchoring strength W is infinite [26]. The calculated LC configuration without considering the third term is well in agreement with experiment results, especially for cells with rubbed alignment layer whose anchoring strength is in order of 10^{-3} J/m^2. However, the anchoring strength of photoalignment layer is not as strong as that of rubbed alignment layer with order of 10^{-5} J m^{-2} [27] so that the last term surely needs to take into account Gibbs free energy to calculate exact electro-optical characteristics. Under a weak anchoring condition, the effective cell gap d increases to $d + b$, where b is the extrapolation length defined as $b = K/W$ (K is elastic coefficient of LC material) [28]. Consequently, electro-optic performances of LC device are strongly affected by magnitude of anchoring energy. In conventional vertical alignment mode where vertically aligned LCs experiences bend deformation by a vertical electric field, K and W are replaced by bend elastic constant K_{33} and W_θ, whereas in the in-plane switching mode where

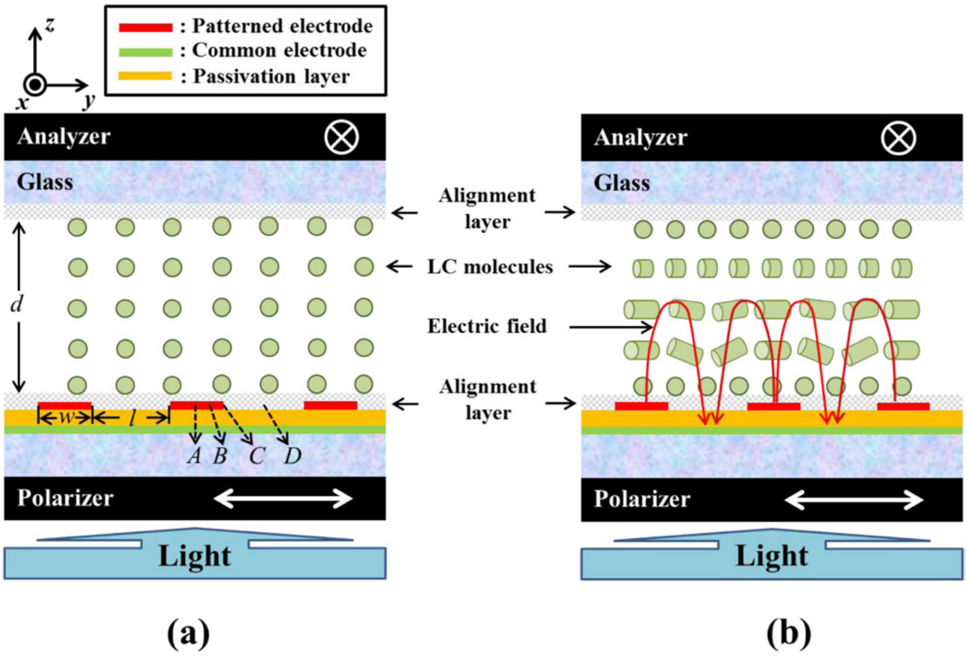

Figure 1. Schematic cell structure with molecular orientation in the fringe-field switching mode: (a) off-state and (b) on-state.

homogenously aligned LCs experiences in-plane rotation by in-plane field both are replaced by K_{22} and W_φ [29, 30]. In the FFS mode, the reorientation of LC by applied fringe-electric field is rather complex as described above and schematically drawn in figure 1(b) such that tilt as well as twist deformation does occur, implying that both W_θ and W_φ need to take into account for calculating electro-optics.

In this study, 2 × 2 extended Jones matrix is applied for an optical transmittance calculation. For the electro-optic calculations, the LC material ($K_{11} = 13.2$ pN, $K_{22} = 6.6$ pN, $K_{33} = 15.4$ pN, $\Delta\varepsilon = 7.9$, $\gamma = 72$ mPa s, $\Delta n = 0.1$ at 587.3 nm) is used and the magnitude of both W_θ and W_φ is varied to investigate its effects on electro-optic performances of a FFS LC cell. The width of patterned electrode and distance between patterned electrodes are 3 μm and 4.5 μm, respectively. The thickness of the passivation layer between patterned and common electrodes is 0.25 μm and d is 3.4 μm. The alignment direction of LC director is 83° with respect to y-direction. The surface pretilt angle for both substrates is 0° since a planar alignment layer with photoalignment process gives rise to almost zero pretilt angle in general [27]. In addition, when calculation normalized transmittance, the T_o is defined as the transmittance of a cell with two parallel polarizers in the voltage-off state.

3. Simulation results and discussion

In order to investigate how electro-optics of the FFS cells are affected by W_θ and W_φ anchoring strength, seven different cases are tested. The first cell is reference with W_θ and W_φ having infinity values such that the easy axis of LC director on each substrate is fixed and cannot be slid regardless of the magnitude of an applied voltage. Six sets of anchoring strengths (W_φ, W_θ) in N m^{-1} $\in$ (10^{-3}, 10^{-3}), (10^{-3}, 10^{-4}), (10^{-4}, 10^{-3}), (10^{-4}, 10^{-4}), (5×10^{-5}, 10^{-3}), (5×10^{-5}, 10^{-4}) have been evaluated and are labelled as No.1…No.6, respectively.

Figure 2 shows the voltage-dependent normalized transmittance (V–T) curves of the FFS cells as a function of magnitude of surface anchoring strengths. The transmittance of a LC cell under No. 1 condition shows 0.653 at 4.2 V and the shape of V–T curve is nearly similar to that of the FFS cell under reference condition (0.654, 4.2 V). The maximum transmittances of the FFS cell under No.3 and No.5 condition are 0.684 at 4.0 V and 0.713 at 3.8 V, respectively. The FFS cell with No.5 condition reduces an operating voltage by 10% compared to the FFS cell under reference condition, and at the same time, the transmittance is also increased by about 4% to 5% by decrease of one order in W_φ. From the results, we could confirm that azimuthal anchoring strength affects the maximum transmittance as well as the threshold voltage (V_{th}) and operating voltage (V_{op}) of an FFS cell.

From the comparison of V–T curves between even and odd numbered cells in which there is only difference by one order of W_θ in each condition, we could confirm that the slope of V–T curves under T_{50} is nearly equal but the maximum transmittance at V_{op} between even and odd numbered cells is quite much different. The transmittance of FFS LC cells with No.2, No.4 and No.6 represents 0.603 at 4 V, 0.627 at 3.8 V and 0.650 at 3.6 V, respectively. The results clearly indicate that the V_{op} is not much affected by the magnitude of W_θ, however, the maximal transmittance of the cells with No. 2, No.4, and No.6 drops by about 8%, 9%, and 10% when the cells are compared with No.1, No.3, and No.5, respectively. The results clearly indicate that the polar anchoring strength strongly plays an important role on transmittance such that higher polar anchoring strength is favoured for higher transmittance at a given azimuthal anchoring strength.

Next, response times of the FFS LC cell under each anchoring condition are calculated. The voltage which shows

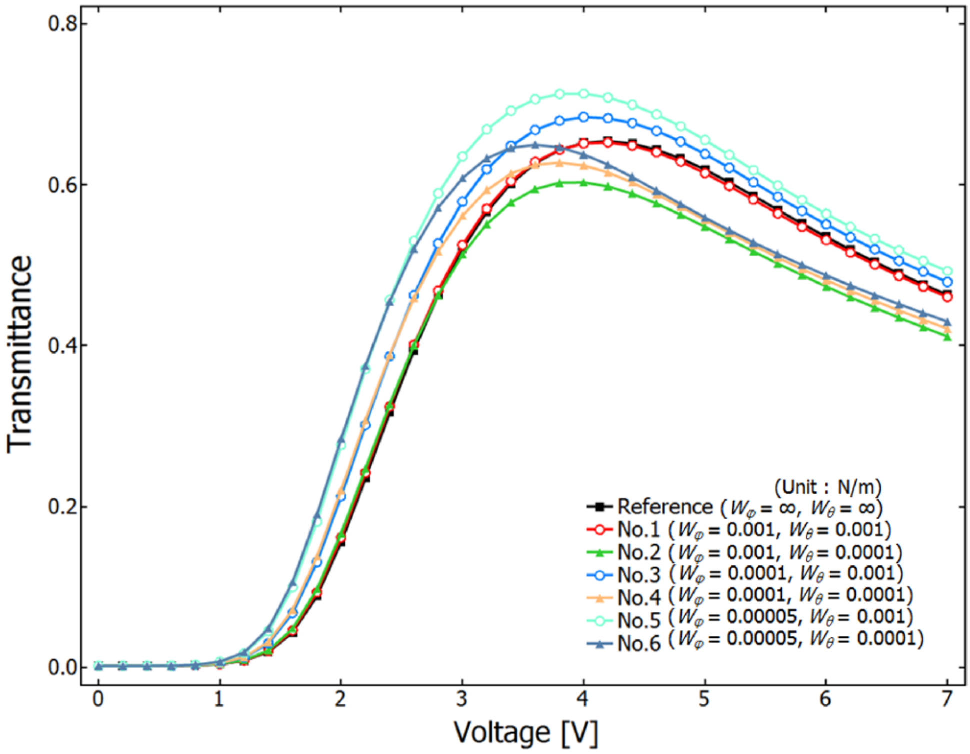

Figure 2. Voltage-dependent transmittance curves in the FFS cells with +LC as a function of the amplitude of anchoring strengths.

90% of maximal transmittance was applied in order to avoid any effects associated with an electro-optic bounce during switching [31]. The rising (τ_r) and falling (τ_d) times are calculated as a time at which the transmittance changes by 80% during switching. The rising (τ_r) and falling (τ_d) times of the reference FFS cell are 21.6 ms and 15.4 ms at 3.4 V, respectively. The cell with No.1 anchoring condition records about the same level of response times ($\tau_r = 22.3$ ms, $\tau_d = 15.4$ ms at 3.3 V) as those with reference anchoring condition. The response times of the FFS cells under No.3 and No.5 anchoring condition are 40.1 ms ($\tau_r = 23.4$ ms and $\tau_d = 16.7$ ms at 3.3 V) and 43.6 ms ($\tau_r = 25.5$ ms and $\tau_d = 18.1$ ms at 3.0 V). The rising time of LC cell is inversely proportional to V^2, and the falling time becomes faster with a strong anchoring condition [32]. Consequently, τ_r and τ_d become slower with decreasing W_φ. On the other hand, the cells with No.2 and No.6 conditions exhibit response times of 38.1 ms ($\tau_r = 23.0$ ms and $\tau_d = 15.1$ ms) and 43.5 ms ($\tau_r = 25.7$ ms and $\tau_d = 17.8$ ms), respectively. Comparing cells between No.1 (No.5) and No.2 (No.6), the effects of W_θ are minimal.

Summarizing what has been observed in V–T curves and response times as a function of magnitude of anchoring strengths, reduction of both W_θ and W_φ is favoured for low operating voltage but increasing W_θ and lowering W_φ are favoured for high transmittance. Especially, weak polar anchoring strength of alignment layers under the same conditions results in significant amount of reduction in maximum transmittance of a FFS mode when a LC with positive dielectric anisotropy (+LC) is used. When considering response times only, especially falling time, strong W is favoured. Consequently, strong W_θ and weak W_φ results in high transmittance and relatively low operating voltage, which is favourable for portable LCDs with low power consumption. However, strong W_θ and strong W_φ are favoured for fast response time and proper transmittance, which is favourable for LC-television application.

In order to analysis why the optical transmittance of the FFS cell with +LC is affected by anchoring energy, we calculate the transmittance along electrode position at V_{op} which shows maximum transmittance T_{100}, as shown in the figure 3(a). The transmittance difference in cells between reference and No.5 is small near edge of electrodes (electrode position C). The initial LC orientation on bottom surface layer at position C under reference anchoring condition is not changed due to the infinite anchoring strength, but the intensity of E-field is enough to rotate the LC director to horizontal E-field direction so that polarization rotation effect is still available. On the other hand, positions A and D as shown in figure 3(a) under No.5 anchoring condition contribute to higher transmittance than that in the conventional FFS cell. In order to understand this behavior in details, azimuthal and tilt angles in reference and No.5 condition are calculated at two electrode positions C and D, as shown in figures 3(b) and (c). The profile of tilt angles in cells of the reference and No.5 is about the same each other implying that the magnitude of W_θ, 10^{-3} is strong enough to give the same profile in tilt angles. On the other hand, the LCs of the FFS cell under No.5 condition are more twisted towards horizontal field direction due to a weaker azimuthal anchoring strength. In addition, LC director at position D where the LCs can be twisted by pure elastic torque of neighbouring LCs due to absence of an E_y rotate more in No. 5 than in the reference due to weak azimuthal anchoring strength.

The electrode width and distance between them is one of the factors for improving the transmittance of the FFS mode.

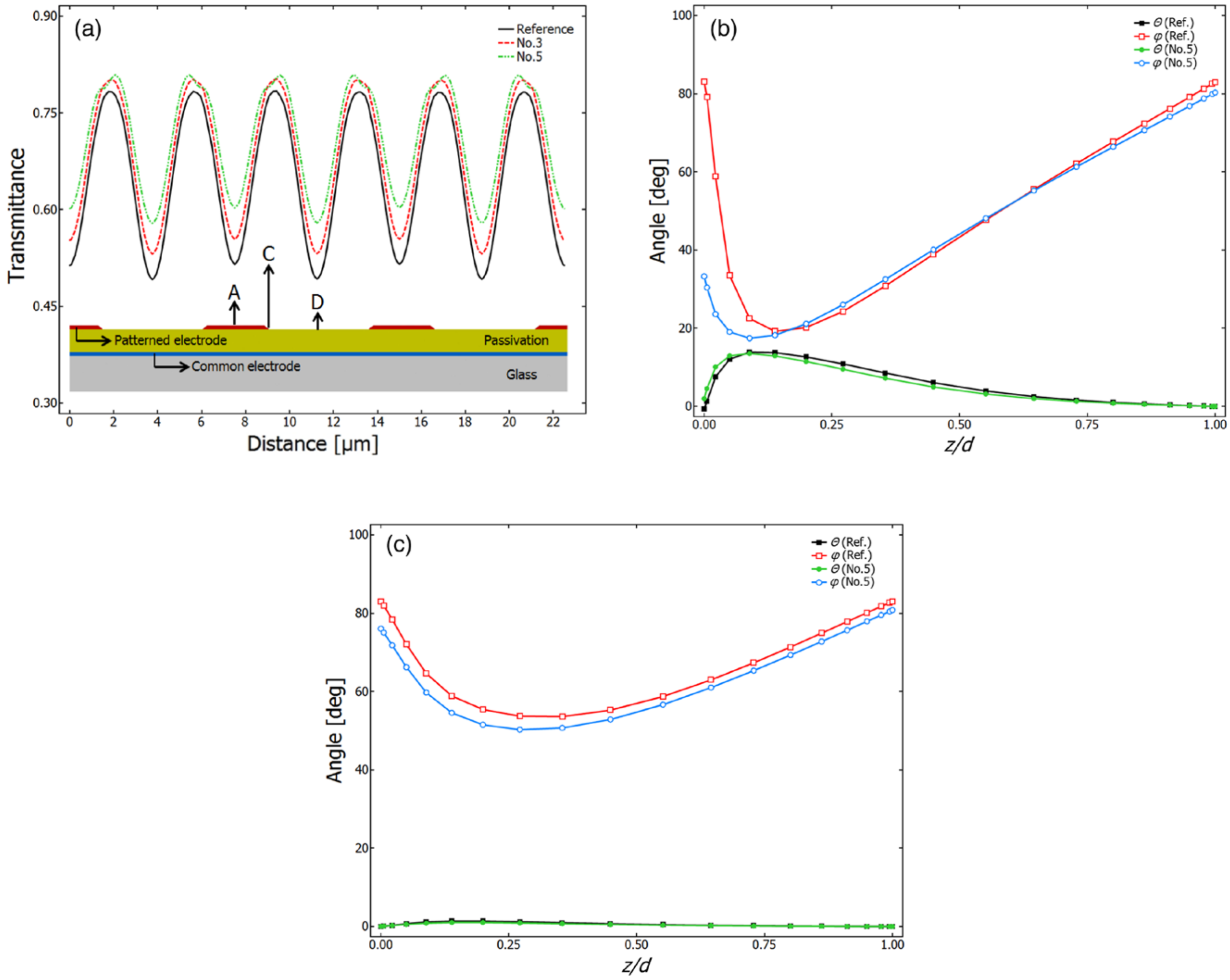

Figure 3. (a) Transmittance profile along y direction at V_{op} in the FFS cells with +LC: reference, No.5 and No.6. Director profile of LC orientation in tilt (θ) and twist (φ) angles is extracted at electrode position C (b) and D (c).

Commonly, the electrode configuration with fine w and l results in higher V_{op} [20, 21]. Figure 4(a) represents the V–T curves of the FFS cell with +LC in different pitch conditions (6, 7.5, 9) in μm with strong anchoring energy of infinity. Here, all other cell parameters are the same as the above except for the electrode pitch and the pitch is defined by summation of w and l. Also, we restrict the width of patterned electrode to 3 μm. As expected, the cell with pitch 6 μm ($w = 3$ μm, $l = 3$ μm) shows the best optical transmittance (0.676) at 4.8 V among all pitch conditions under strong anchoring condition. In order to confirm the effect of anchoring condition under different pitches, we apply the anchoring condition No. 5 to each cell. As expected, the V–T curves shift to the left and also exhibit higher transmittance in all cells with weaker azimuthal anchoring conditions compared to the cells with strong anchoring conditions, as shown in figures 4(a) and (b). The transmittance of the pitch 6 μm records 0.730 at 4.4 V, in which the transmittance is improved by about 8% and the V_{op} is decreased by about 9%, while the increase rate of transmittance for the cell with the pitch 9.0 μm is about 10%. The results clearly indicate that the effects of W_φ on V–T curves of the FFS cells are still valid irrespective of the electrode pitch.

Next, the effects of W_θ on V_{op} and transmittance have been evaluated, as shown in figures 4(c) and (d). Here, two cases with anchoring conditions of No.5 and No.6 (same magnitude of W_φ but W_θ of No.5 is one order higher than that of No.6) have been compared. The V_{op} and maximum transmittance of the FFS cells under No.6 condition are decreased compared to those with No.5. The maximum transmittances of the FFS cells with No.6 are 0.656, 0.650 and 0.626 for pitches 6 μm, 7.5 μm, 9 μm, respectively. The transmittance difference between two FFS cells with No.5 and No. 6 anchoring condition is about 11% and 9% for pitches 6 and 9 μm, respectively. Consequently the results clearly indicate that the alignment layer with strong W_φ is favoured for achieving high transmittance, irrespective of pitch lengths.

Magnitude of surface anchoring energy of an alignment layer strongly affects electro-optics of the FFS cell. At the same time, the cell gap also strongly affects transmittance and response time of an FFS cell. The transmittance in an FFS mode can be improved by increasing a cell gap which affects the mauguin parameter for wave guiding in twisted LC configuration at electrode position C and elastic torque between neighbouring LCs in bulk LC layer at electrode

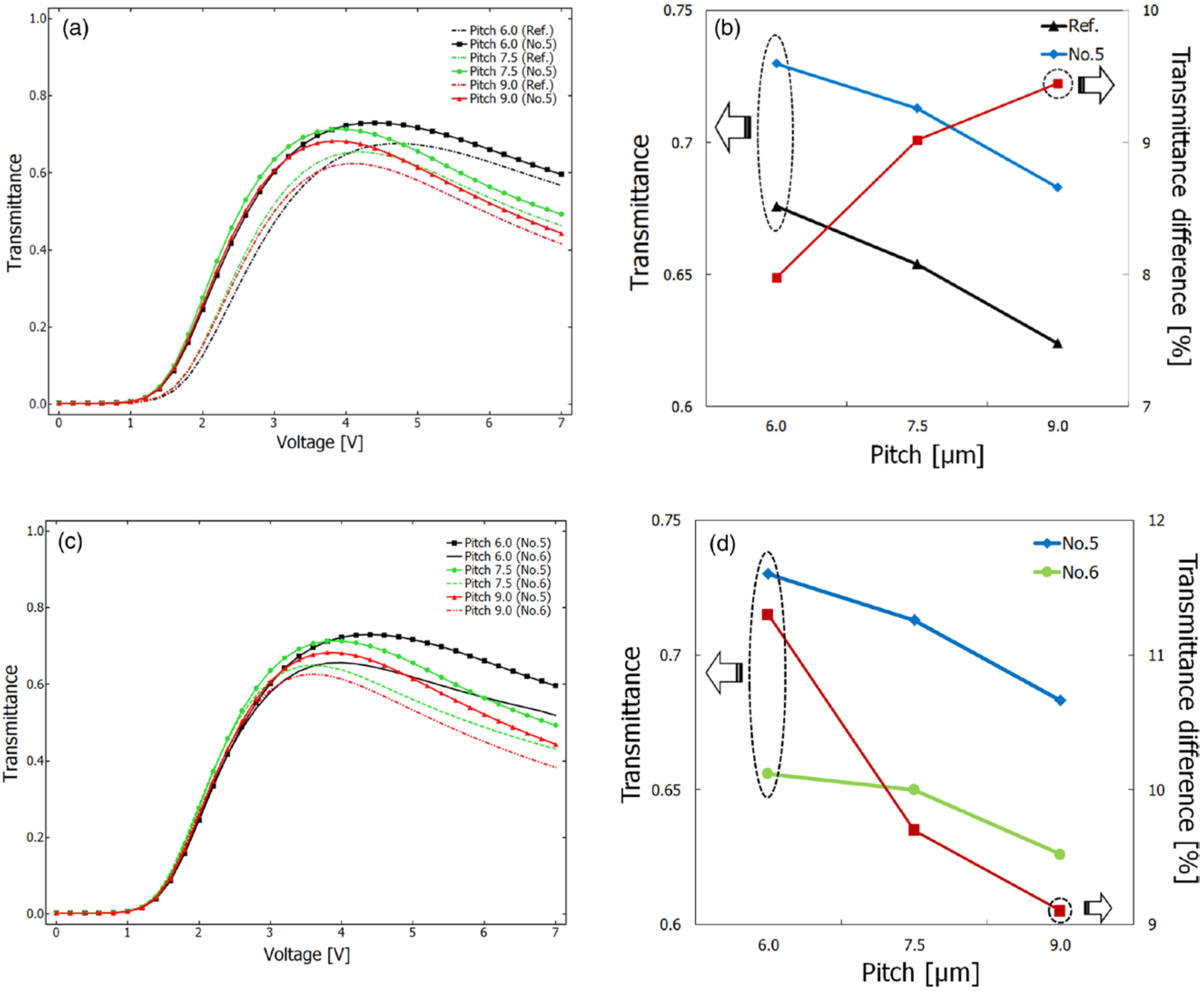

Figure 4. Voltage-dependent transmittance curves for the FFS cells with +LC as a function of pitches in different anchoring conditions: (a) reference and No.5 and (b) its summary of maximum transmittance and transmittance difference between reference and No.5. Voltage-dependent transmittance curves for the FFS cells with +LC as a function of pitches and amplitudes of polar anchoring conditions: (c) No.5 and No.6, and (d) its summary of maximum transmittance and transmittance difference between No.5 and No.6.

positions A and D, as explained in the switching principle [18, 19]. Figures 5(a) and (b) shows *V–T* curves for the FFS cells with +LC as a function of cell gaps with two anchoring conditions: ref. and No.3. As the cell gap decreases, the transmittance decreases but its decreasing ratio can be smaller with anchoring condition No.3 such that the transmittance of the FFS cell at $d = 2.8\ \mu$m can be improved by 6.5% compared to the cell with strong anchoring condition. Figure 5(c) shows the transmittance profile along *y* direction, clearly showing that the cell with anchoring condition No.3 exhibits a better transmittance mainly at electrode positions A, C, and D compared to those with strong anchoring condition. In the FFS cell, its decay response time is mainly determined by LC's elastic restoring force proportional to $\gamma\ d^2/K_{22}$. Therefore, reduction of *d* is inevitable to achieve a very fast decay response time, which results in a decrease in transmittance. Conclusively speaking, controlling anchoring energy of an alignment layer while decreasing the *d* is required to achieve a high transmittance as well as a fast response time in the FFS cell.

The transmittance of the FFS mode also depends on the sign of dielectric anisotropy of LC material such that the LC with negative dielectric anisotropy (−LC) is higher than that of +LC [20, 21, 33–35]. In the FFS mode, the +LC will try to orient parallel to the field; however, the −LC orients perpendicular to the electric field. In other words, the +LC will tilt upward highly along the fringe field at electrode position B whereas the fringe field at that position will generate much less tilt angle with −LC [23]. Therefore, in order to understand clearly how the observed electro-optic characteristics with +LC might be changed with −LC depending on anchoring conditions of an alignment layer, we apply the same anchoring strength conditions to the FFS cells with −LC. In this study, the −LC material has physical properties, such as dielectric anisotropy $\Delta\varepsilon = -4.1$, rotational viscosity $\gamma = 143$ mPa s, $\Delta n = 0.09763$ at 633 nm, $K_{11} = 14.5$ pN, $K_{22} = 7.25$ pN and $K_{33} = 15.3$ pN. The initial tilt angle and rubbing angle for the FFS cell with −LC is 2° and 7° with respect to *y* direction, respectively and *d* is 3.4 μm. The other cell parameters are the same as figure 2.

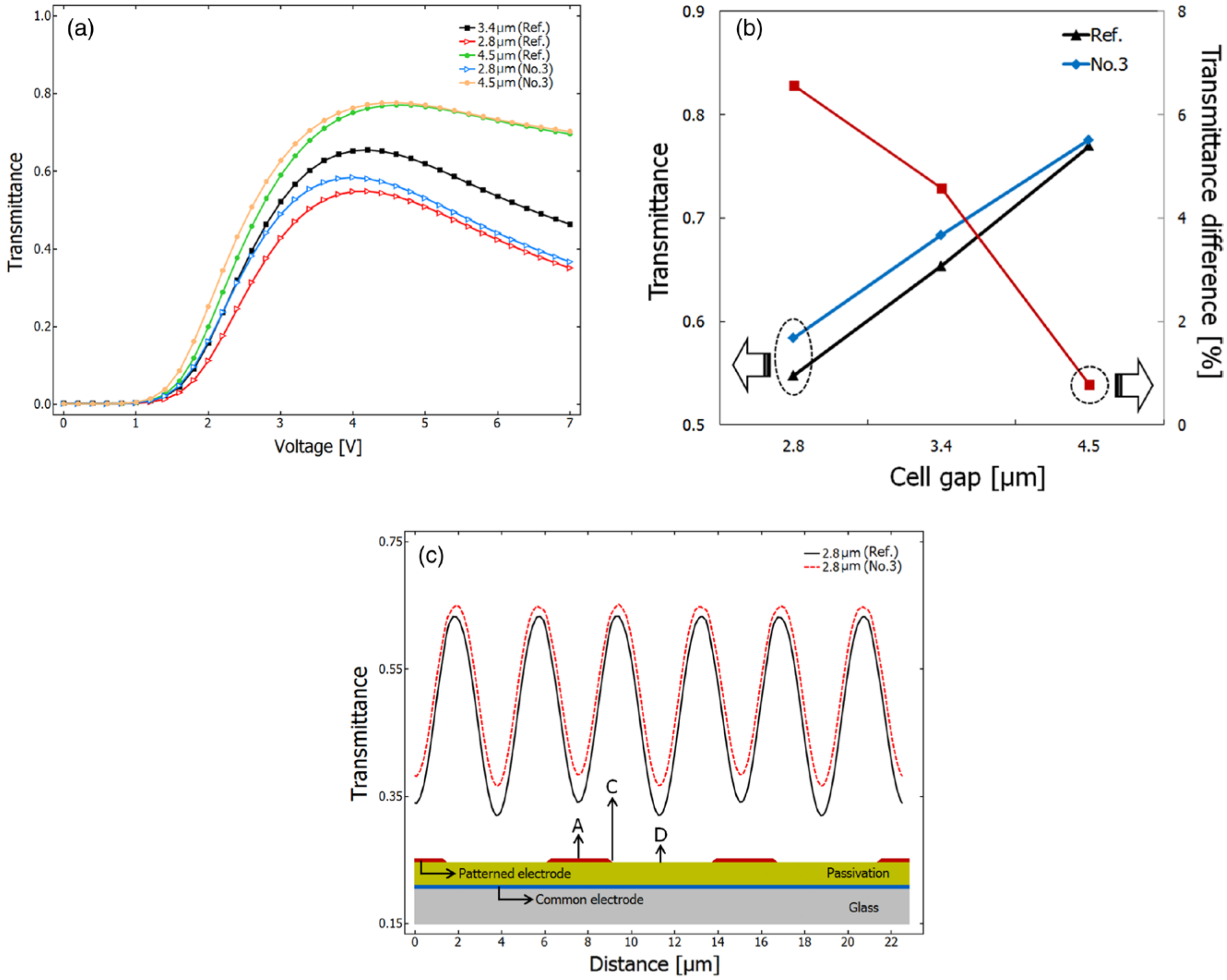

Figure 5. (a) Voltage-dependent transmittance curves of the FFS cells with +LC as a function of cell gaps with two anchoring conditions: reference and No.3, (b) its summary of maximum transmittance and transmittance difference between reference and No.3, and (c) transmittance profile along y direction at V_{op} in the FFS cells with +LC under anchoring strengths reference and No.3 anchoring strength when $d = 2.8\ \mu$m.

Figure 6(a) indicates the V–T curves of the FFS cells with −LC as a function of surface anchoring strengths. As clearly indicated, the V–T curves shifts to the left and the transmittance increases as the amplitude of the W_φ decreases from 10^{-3} to 10^{-5}, which follows the same behavior of those of +LC. However, the maximum transmittance of the FFS cell with −LC is not much affected by one order decrease of W_θ, unlike the FFS cells with +LC. Figure 6(b) shows the electrode-position dependent transmittance along y direction for two cells with anchoring conditions No.5 and No.6. As clearly indicated, the transmittance difference between the two cells exists slightly at electrode position C but it is almost negligible at electrode positions A and D where the rotating angle of LC director is determined by elastic torque between neighbouring molecules. Conclusively speaking, when a −LC is used in the FFS mode, the tilt angle at electrode position B is much smaller compared to that with +LC because the vertical component E_z of a fringe-electric field suppresses a tilt angle of LC director so that the magnitude of W_θ affects the maximal transmittance of the FFS cell much less than that with +LC. Finally, the transmittance and the transmittance difference of the FFS cells with −LC depending on anchoring conditions are summarized in figure 6(c). As indicated, the transmittance can be improved more than 6% with anchoring condition No.5 compared to that with Reference, however, it is about 1% between two cells No.5 and No.6, suggesting that controlling azimuthal anchoring energy rather than polar anchoring energy is more important to improve a transmittance and lower an operating voltage in the FFS cell with −LC.

4. Conclusion

In this paper, we studied how azimuthal and polar anchoring strength of an alignment layer affects electro-optic performance of the FFS mode with numerical simulation. From the investigation, we confirm that the smaller azimuthal anchoring energy, its transmittance becomes higher and operating voltage decreases irrespective of cell gaps, electrode structures, and sign of dielectric anisotropy. Very interestingly, the polar anchoring strength in the FFS cell with +LC can considerably have an effect on the maximum transmittance; however, its effect becomes negligible in the FFS cell with −LC.

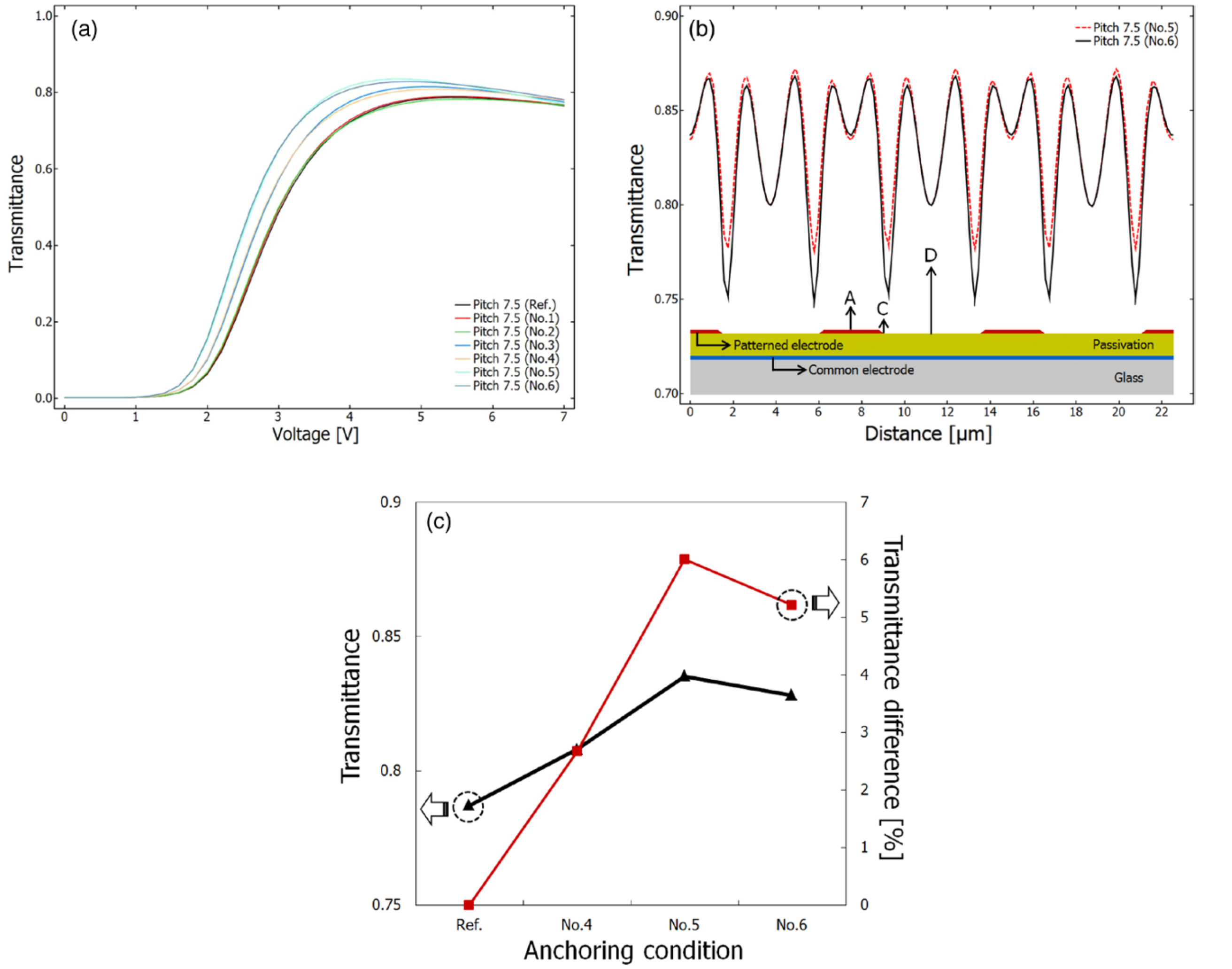

Figure 6. (a)Voltage-dependent transmittance curves of the FFS cells with −LC as a function of surface anchoring strengths, (b) transmittance profile along y direction at V_{op} in the FFS cells with −LC under anchoring conditions of No.5 and No.6, and (c) maximum transmittance and transmittance difference between reference and various anchoring conditions of the FFS cells with −LC.

This result is highly important to design an alignment layer to maximize the light efficiency of an FFS-LCD.

Acknowledgments

This research was supported by Basic Science Research Program through the National Research Foundation of Korea(NRF) funded by the Ministry of Education(2013R1A1A2005630).

References

[1] Schadt M and Helfrich W 1971 *Appl. Phys. Lett.* **18** 127
[2] Oh-e M and Kondo K 1995 *Appl. Phys. Lett.* **67** 3895
[3] Takeda A, Kataoka S, Sasaki T, Chida H, Tsuda H, Ohmuro K, Sasabayashi T, Koike Y and Okamoto K 1998 *SID Dig. Tech. Papers.* **29** 1077
[4] Lyu J J, Hyang J S, Kim Y and Lee S H 2007 *J. Disp. Technol.* **3** 404
[5] Lee S H, Lee S L and Kim H Y 1998 *Appl. Phys. Lett.* **73** 2881
[6] Kang W S, Moon J-W, Lee J-H, Kim B-K, Choi H C, Lee S H and Lee G-D 2011 *J. Opt. Soc. Korea* **15** 161
[7] Dozov I, Nobili M and Durand G 1997 *Appl. Phys. Lett.* **70** 1179
[8] Tie W, Jeong I H, Jang I W, Han J S, Liu Y, Li X-D, Lee M-H, Jeong K-U and Lee S H 2014 *Liq. Cryst.* **41** 1057
[9] Schadt M, Schmitt K, Hozinkov V and Chigrinov V 1992 *Japan. J. Appl. Phys.* **31** 2155
[10] Gibbons W, Shannon P, Sun S and Swetlin B 1991 *Nature* **351** 49
[11] Ichimura K, Suzuki Y, Seki T, Hosoki A and Aoki K 1988 *Langmuir* **4** 1214
[12] Ahn H J, Lim C S, Kim D J, Lee J H, Park H J, Lee S B, Woo J W, Shin W S and Jun M C 2012 *SID Int. Symp. Dig. Tech. Papers* **43** 1432
[13] Goto K, Yamanouchi H, Ashizawa R, Mandai A, Nagi T, Minami S, Tsutsui K, Ishikawa M, Kondo M and Kawatsuki N 2013 *SID Int. Symp. Dig. Tech. Papers* **44** 537
[14] Masahito O, Kim D and Shen Y R 2001 *J. Chem. Phys.* **115** 5582
[15] Jung S H, Kim H Y, Kim J H, Nam S H and Lee S H 2004 *Japan. J. Appl. Phys.* **43** 1028
[16] Oh S M, Kim S J, Lee M H, Seo D S and Lee S H 2005 *Mol. Cryst. Liq. Cryst.* **433** 97
[17] Ryu J W, Lee J Y, Kim H Y, Park J W, Lee G D and Lee S H 2008 *Liq. Cryst.* **35** 407

[18] Jung S H, Kim H Y, Lee M-H, Rhee J M and Lee S H 2005 *Liq. Cryst.* **32** 267
[19] Kim S J, Kim H Y, Lee S H, Lee Y K, Park K C and Jang J 2005 *Japan. J. Appl. Phys.* **44** 6581
[20] Yun H J, Jo M H, Jang I W, Lee S H, Ahn S H and Hur H J 2012 *Liq. Cryst.* **39** 1141–8
[21] Jo M H, Yun H J, Jang I W, Jeong I H, Lee S H, Cho S H, Ahn S H and Heo H J 2013 *Liq. Cryst.* **40** 368–73
[22] Ryu J W, Lee J Y, Lim Y J, Kim K-M, Lee G-D and Lee S H 2007 *Mol. Cryst. Liq. Cryst.* **476** 239
[23] Jung J H, Ha K S, Chae M, Srivastava A K, Lee S-E, Lee H K and Lee S H 2010 *J. Kor. Phys. Soc.* **56** 548
[24] Leslie F M 1968 *Arch. Ration. Mech. Anal.* **28** 265–83
[25] Kang W S, Joo W Y, Hur S Y, Han H Y, Lee G-D, Youn H J and Jeong B 2010 *J. Kor. Phys. Soc.* **57** 752
[26] Mori H, Gartland E C Jr, Kelly J R and Bos P J 1999 *Japan. J. Appl. Phys.* **38** 135
[27] Kimura M, Nakata S, Makita Y, Matsuki Y, Kumano A, Takeuchi Y and Yokoyama H 2001 *Japan. J. Appl. Phys.* **40** L352
[28] Yoneya M, Iwasaki K, Tomioka Y and Kondo K 1999 *Appl. Phys. Lett.* **74** 803
[29] Nie X, Lu R, Xianyu H, Wu T X and Wu S-T 2007 *J. Appl. Phys.* **101** 103110
[30] Lee S H, Lee S L, Kim H Y and Eom T Y 1999 *J. Kor. Phys. Soc.* **35** S1111–4
[31] Ha K S, Woo C W, Bhattacharyya S S, Yun H J, Jin H S, Jang Y-K and Lee S H 2012 *Liq. Cryst.* **39** 39
[32] Xu D, Peng F, Tan G, He J and Wu S-T 2015 *J. Appl. Phys.* **117** 203103
[33] Kim H Y, Nam S-H and Lee S H 2003 *Japan. J. Appl. Phys.* **42** 2752
[34] Kim D H, Lim Y J, Kim D E, Ahn S H and Lee S H 2014 *J. Inform. Disp.* **15** 99–106
[35] Chen H, Peng F, Hu M and Wu S-T 2015 *Liq. Cryst.* at press (doi: 10.1080/02678292/2015/1061714)